

[Click for updates](#)

Remote Sensing Letters

Publication details, including instructions for authors and
subscription information:

<http://www.tandfonline.com/loi/trsl20>

Evapotranspiration in Korea estimated by application of a neural network to satellite images

Jong-Min Yeom^a, Chang-Suk Lee^b, Soo-Jae Park^c, Jae-Hyun Ryu^d,
Jae-Jin Kim^e, Hyun-Cheol Kim^f & Kyung-Soo Han^b

^a Earth Observation Research Team, Korea Aerospace Research
Institute, Daejeon, Republic of Korea

^b Department of Spatial Information Engineering, Pukyong
National University, Busan, Republic of Korea

^c Global Environment System Research Division, National Institute
of Meteorological Research (NIMR), Seogwipo-si, Jeju-do, Republic
of Korea

^d National Meteorological Satellite Center (NMSC), Korea
Meteorological Administration, Jincheon-gun, Republic of Korea

^e Department of Environmental Atmospheric Sciences, Pukyong
National University, Busan, Republic of Korea

^f Division of Polar Ocean Environment, Korea Polar Research
Institute, Incheon, Republic of Korea

Published online: 01 May 2015.

To cite this article: Jong-Min Yeom, Chang-Suk Lee, Soo-Jae Park, Jae-Hyun Ryu, Jae-Jin Kim, Hyun-Cheol Kim & Kyung-Soo Han (2015) Evapotranspiration in Korea estimated by application of a neural network to satellite images, *Remote Sensing Letters*, 6:6, 429-438, DOI: [10.1080/2150704X.2015.1041169](https://doi.org/10.1080/2150704X.2015.1041169)

To link to this article: <http://dx.doi.org/10.1080/2150704X.2015.1041169>

PLEASE SCROLL DOWN FOR ARTICLE

Taylor & Francis makes every effort to ensure the accuracy of all the information (the "Content") contained in the publications on our platform. However, Taylor & Francis, our agents, and our licensors make no representations or warranties whatsoever as to the accuracy, completeness, or suitability for any purpose of the Content. Any opinions and views expressed in this publication are the opinions and views of the authors, and are not the views of or endorsed by Taylor & Francis. The accuracy of the Content should not be relied upon and should be independently verified with primary sources

of information. Taylor and Francis shall not be liable for any losses, actions, claims, proceedings, demands, costs, expenses, damages, and other liabilities whatsoever or howsoever caused arising directly or indirectly in connection with, in relation to or arising out of the use of the Content.

This article may be used for research, teaching, and private study purposes. Any substantial or systematic reproduction, redistribution, reselling, loan, sub-licensing, systematic supply, or distribution in any form to anyone is expressly forbidden. Terms & Conditions of access and use can be found at <http://www.tandfonline.com/page/terms-and-conditions>

Evapotranspiration in Korea estimated by application of a neural network to satellite images

Jong-Min Yeom^a, Chang-Suk Lee^b, Soo-Jae Park^c, Jae-Hyun Ryu^d, Jae-Jin Kim^e,
Hyun-Cheol Kim^f, and Kyung-Soo Han^{b*}

^aEarth Observation Research Team, Korea Aerospace Research Institute, Daejeon, Republic of Korea; ^bDepartment of Spatial Information Engineering, Pukyong National University, Busan, Republic of Korea; ^cGlobal Environment System Research Division, National Institute of Meteorological Research (NIMR), Seogwipo-si, Jeju-do, Republic of Korea; ^dNational Meteorological Satellite Center (NMSC), Korea Meteorological Administration, Jincheon-gun, Republic of Korea; ^eDepartment of Environmental Atmospheric Sciences, Pukyong National University, Busan, Republic of Korea; ^fDivision of Polar Ocean Environment, Korea Polar Research Institute, Incheon, Republic of Korea

(Received 28 December 2014; accepted 7 April 2015)

Previous biophysical and empirical models of evapotranspiration retrieval are difficult to parameterize because of the effects of the nonlinear biophysics of plants, terrestrial and solar radiation and soils, despite attempts made using various satellite products. In this study, the multilayer feed-forward neural network approach with Levenberg–Marquardt back propagation (LM-BP) was used to successfully estimate evapotranspiration using the input of various satellite-based products. When applying neural network training, value-added satellite-based products such as normalized difference vegetation index (NDVI), normalized difference water index (NDWI), land surface temperature (LST), air temperature and insolation are used instead of only spectral information from satellite sensors to reflect the spatial representativeness of the neural network. The evapotranspiration estimated from the neural network with input parameters showed better statistical accuracy than the MODIS products (MOD16) and Priestley–Taylor methods when compared with ground station eddy flux measurements, which were considered as reference data. Additionally, the temporal variation in neural network evapotranspiration well reflected seasonal patterns of eddy flux evapotranspiration, especially for the high cloudiness in the summer season.

1. Introduction

Global warming due to enhanced greenhouse effects is considered a major cause of changes in various climatic variables, such as precipitation, evapotranspiration (ET) and net terrestrial and global solar radiation (Goyal 2004). ET, which is the process of converting water into water vapour via surface evaporation and plant transpiration, is an essential parameter for linking terrestrial water, carbon and surface energy exchanges (Wang and Dickinson 2012). ET is also a major factor of the post-precipitation hydrological cycle process, and it determines the plant water requirement by returning more than 60% of the precipitation that reaches land back to the atmosphere (Korzoun and Sokolov 1978; L'vovich et al. 1990). Although spatially reliable information on ET is required to understand the hydrological cycle and carbon exchange between the surface

*Corresponding author. Email: kyung-soo.han@pknu.ac.kr

and atmosphere, it is difficult to obtain in practice because of cost problems associated with the collection of sufficient field observations to parameterize all ecosystem types, which hampers the accurate quantification of ET. Here, remote sensing comes into play as a cost-effective tool/alternative for estimating ET. Generally, a combination of biophysical models and satellite remote sensing is used for estimating and scaling eddy flux ET measurements to large areas (Mu, Zhao, and Running 2011). It is important to interpret the relationship between eddy flux measurements and satellite information with biophysical models or statistical approaches to spatial hydrological information. Kaminsky, Barad, and Brown (1997) and Cincotti, Marchesi, and Serri (1996) regarded the neural network approach to be more effective than traditional statistical techniques for use with remotely sensed data. In this study, the Levenberg–Marquardt neural network (Levenberg 1944; Marquardt 1963) technique is applied to satellite remote sensing to estimate ET by using surface flux measurements. When training the neural network for ET, value-added satellite-based products that are highly related with ET estimation are retrieved with polar and geostationary satellites and used as input parameters.

2. Materials and methods

2.1. Data

For the performance of the neural network, the following remote sensing-based input parameters were considered and explored for a training network: date, normalized difference vegetation index (NDVI), normalized difference water index (NDWI), IR1 brightness temperature (10.3 μm), IR2 brightness temperature (11.5 μm), land surface temperature (LST), air temperature (T_a) and insolation (R_s). When we determined the remote-sensing-based input parameters, ET-related parameters were selected carefully based on previous studies (Wanchang, Yamaguchi, and Ogawa 2000; Sánchez et al. 2007; Gao, Long, and Li 2008; Mu, Zhao, and Running 2011; Sun et al. 2012). Date is used to reflect temporal variation in the Sun–Earth distance, which determines the extraterrestrial solar radiance. The NDVI and NDWI, which are estimated primarily using the atmospherically corrected surface reflectance, were explored to evaluate the status of vegetation growth and vegetation water stress, respectively. The vegetation indices were selected instead of using the raw near infrared (NIR) and red bands reflectance to reduce temporally dependent atmospheric effects by using actual information on vegetation and to reflect the spatial variation in vegetation, as the normalized band ratios for red, NIR (0.86 μm) and NIR (1.24 μm) are useful for interpreting the characteristics of vegetation using satellite data (Rouse et al. 1974; Gao 1996). Additionally, for more reliable value-added satellite products, atmospheric correction with the second simulation of the satellite signal in the solar spectrum (6S) code and the semi-empirical bidirectional reflectance distribution function (BRDF) model are applied to the observed top-of-atmosphere spectral images by considering two different observation characteristics between polar and geostationary satellites (Roujean, Leroy, and Deschamps 1992; Vermote et al. 1997). In the case of vegetation indices for plant transpiration, surface BRD effects, which could be relative solar-target-sensor fluctuation errors, are carefully removed with the BRDF model based on MODIS nadir BRDF-adjusted reflectance products composite criteria (Lucht, Schaaf, and Strahler 2000; Schaaf et al. 2002). To interpret the evaporation from soil and to estimate ET, water storage under canopy height and transpiration of vegetation, LST, T_a , IR1 band and IR2 band were used as input parameters in a neural network. When using thermal channels from satellite observations, two satellite products are used to interpret the complicated temperature-based evaporation and transpiration by canopy interception and storage: the polar-orbiting MODIS and geostationary Communication, Ocean

and Meteorological Satellite (COMS). In this study, we estimated the hourly R_s , one of the main energy sources for ET, using geostationary COMS MI images to reflect real-time variation in incident radiance on the canopy (Yeom and Han 2010). Basically, most ET models combined with satellite imagery have used empirical models such as linear regression, climate values, etc., due to the complex atmospheric physical processes, especially for the cloud effect (Heermann, Harrington, and Stahl 1985; Kizu 1998; Isikwue, Amah, and Agada 2012). This study used a physical model that considered atmospheric effects and constituents, such as Rayleigh scattering, water vapour and total ozone for reliable estimation of R_s . By combining a physical model and satellite imagery, cloud attenuation of irradiance with high temporal variation can be reflected in the final ET retrieval. The physical model for R_s is briefly described as follows (Kawamura, Tanahashi, and Takahashi 1998):

$$R_s = S_I + S_R + S_A \quad (1)$$

$$R_s = (S_I + S_R + S_A) \times (CF) \quad (2)$$

Here, R_s , S_I , S_R , S_A and CF are the total insolation, direct irradiance, diffuse irradiance due to Rayleigh scattering, diffuse irradiance due to scattering by aerosols and cloud factor (CF), respectively. Equations (1) and (2) are executed separately depending on whether cloud exists. For cloud pixels, CF , which is the amount of attenuation due to cloud, is multiplied by the clear-sky total R_s in Equation (2). The R_s from COMS MI integrated insolation hourly based measurement during the daytime is used as the daily value. Finally, the estimation methods used for the input parameters are presented briefly in Table 1. The data used were acquired over the Korean Peninsula from 1 April 2011 to 31 December 2012.

A true ET value is a necessary parameter to determine final network weights and biases when training a neural network. Field-observed values from a flux tower were considered true values of ET. Field-measured ET values were collected from a 40 m high tower at the KoFlux Seolmacheon site (SMK) located at Paju, Korea (37° 56' 19" N, 126° 57' 16" E) and a 10 m high tower at the KoFlux Cheongmicheon farmland site (CFK) located at Yeosu, Korea (37° 9' 35" N, 127° 39' 10" E). Those sites are part of the KoFlux network coordinated under AsiaFlux, which is dedicated to measuring and studying water, carbon and energy fluxes continuously in key ecosystems of monsoonal Asia. Detailed information about the KoFlux SMK (mixed forest) and CFK (rice paddy) sites is summarized in Table 2. In this study, we selected two different land cover types for estimating ET with the neural network, using mixed forest at SMK site and

Table 1. Estimation methods of input parameters used in this study.

Input parameter	Method	Developed by	Temporal/spatial resolution
Date	Julian day		Day
NDVI	$(\text{NIR}_{0.86 \mu\text{m}} - \text{Red}) / (\text{NIR}_{0.86 \mu\text{m}} + \text{Red})$	Rouse et al. (1974)	Daily/1 km
NDWI	$(\text{NIR}_{0.86 \mu\text{m}} - \text{NIR}_{1.24 \mu\text{m}}) / (\text{NIR}_{0.86 \mu\text{m}} + \text{NIR}_{1.24 \mu\text{m}})$	Gao (1996)	Daily/1 km
IR1	Brightness temperature at 10.3 μm		Hourly/1 km
IR2	Brightness temperature at 11.5 μm		Hourly/1 km
LST	MOD11A1, MYD11A1	Wan et al. (2002)	Daily/1 km
T_a	Regression method with MOD11	Han, Viau, and Anctil (2004)	Daily/1 km
R_s	Physical model	Yeom and Han (2010)	Hourly/1 km

Table 2. Detailed characteristics of the KoFlux sites used for estimating ET.

AsiaFlux site code	SMK (KoFlux Seolmacheon site)	CFK (Cheongmicheon Farmland site)
Location	Paju, South Korea	Yeoju, South Korea
Position	37° 56' 19" N, 126° 57' 16" E	37° 9'35" N, 127° 39' 10" E
Elevation	269 m above sea level	141 m above sea level
Slope	N/A	0°
Terrain type	Complex	Flat
Climate	Temperate (snow – winter dry – hot summer)	Warm Continental Climate (Dwa)
Mean annual air temperature	11.5°C	11.5°C
Mean annual precipitation	1332 mm	1170 mm
Vegetation type	Mixed forest	Rice paddy
Canopy height	15 m	~1 m

validating the neural network performance using a rice paddy at the CFK site to examine the spatial representativeness problem. Vegetation at the SMK site consists of mixed forest, and the site has a complex terrain type, whereas the CFK rice paddy site is flat terrain with mixed land cover, such as farm roads and houses.

The mean annual air temperature at both the SMK and CFK sites is 11.5°C, and the respective mean annual precipitation is 1332 and 1170 mm, respectively. Eddy correlation flux measurements of ET at the KoFlux have been collected since 2011. Hourly measured flux data at KoFlux during 2011 were aggregated to the daily measurements to correlate with the MODIS and COMS MI image-based products.

Finally, the presented input parameters are matched temporally with eddy correlation flux measurements to consider the seasonal variation in ET.

2.2. Neural network for estimating evapotranspiration

In this study, a multilayer neural network consisting of an input layer, an output layer and a hidden layer is used (Figure 1), because three layers, including one hidden layer, is sufficient to approximate any complex nonlinear function (Coulbaly, Anctil, and Bobée 2000; Yeom et al. 2008). When determining the appropriate number of hidden layers, trial-and-error testing was performed by changing the number of hidden layers from 1 to 30 to make network learning efficient. For neural network training, the Levenberg–Marquardt back propagation (LM-BP) algorithm was selected because it provides a numerical solution to the problem of minimizing the sum of nonlinear least squares between observed and predicted outputs in an iterative manner (Levenberg 1944; Marquardt 1963). The Levenberg–Marquardt algorithm blends the steepest-descent method and the Gauss–Newton algorithm. It inherits the speed advantage of the Gauss–Newton algorithm and the stability of the steepest-descent method (Yu and Wilamowski 2011).

Before training the network, we estimated various input parameters using MODIS products (MOD09, MYD09, MOD11A1 and MYD11A1) and COMS MI products (IR1 band, IR2 band, R_s). Surface meteorological measurements were also used to assist estimation of input parameters. The temporally matched dataset used to estimate ET was split into three parts: a training dataset (50% of the data) to determine network weights and biases, a validation dataset (25% of the data) to evaluate network performance and decide when to

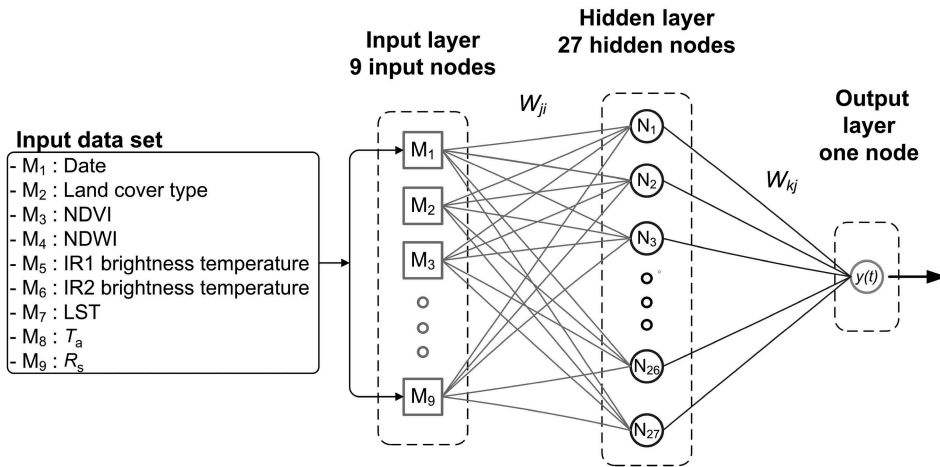


Figure 1. The neural network structure consisting of input, hidden and output layers. M_i ($i = 1, \dots, 9$) are the input nodes and N_j ($j = 1, \dots, 27$) are the hidden nodes. W_{ji} ($i = 1, \dots, 9; j = 1, \dots, 27$) are the first neuron weights between the input nodes and hidden nodes and W_{kj} ($j = 1, \dots, 27; k = 1$) are the second neuron weights between hidden nodes and output node.

stop training and a test dataset (the remaining 25% of the data) to validate the effectiveness of the early stopping criterion and evaluate network operations on the dataset not used in training and validation (Prechelt 1998; Yeom and Han 2010). Each separate dataset still reflected the temporal variation by selecting a regular series. In this study, to avoid overfitting the network training, an early stopping method was applied using a validation dataset. Neural network training was stopped when the relative validation error increased, so we could use a complicated neural network without overfitting (Yeom et al. 2008).

3. Results

Twenty-seven hidden layers were determined by the trial-and-error method for an accurate estimate of ET over the SMK mixed forest site. We compared composited daily ET eddy flux measurements and modelled ET values from the LM-BP neural network using only a test dataset during the study, as shown in Figure 2(a). Additionally, for comparative analysis, the MODIS ET (MOD16) (Mu, Zhao, and Running 2011) and Priestley–Taylor methods (Priestley and Taylor 1972) are estimated and compared with the ET eddy flux measurement for the same period. In Figure 2(a), a scatterplot of ET (red circles) estimated from the LM-BP neural network showed the best results compared with the other methods: the correlation coefficient (r), root mean square error (RMSE) and mean bias error (MBE) were 0.958, 0.3555 mm day⁻¹ and -0.042 mm day⁻¹, respectively (Table 3). Although the MODIS ET products (blue circles) were distributed mostly along the reference line, the R (0.847) and RMSE values (0.650 mm day⁻¹) showed lower accuracy in comparison with our neural network results. The Priestley–Taylor ET (grey circles) had the worst accuracy. Considering the number of collaborated data samples, the neural network LM-BP method is sufficiently powerful to predict the nonlinear relationships of ET without any explicit knowledge of the physical behaviour of the system. In this study, to examine the problem of the spatial representativeness of neural-network-based ET, a temporally matched dataset from the CFK farmland site was used as a validation study area. When estimating ET at the CFK site to examine the spatial applicability of the neural network, we simply used the determined neural

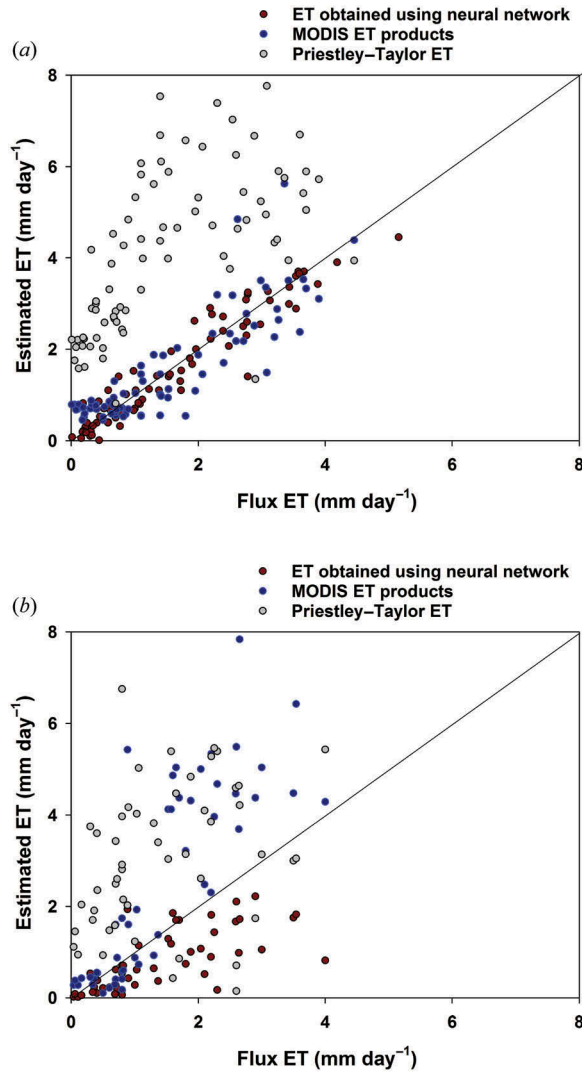


Figure 2. Scatterplots of ET estimated from MODIS (blue circles), Priestley–Taylor methods (grey circles) and the L-BP neural network (red circles) compared with the flux ET over the Seolmacheon (a) and Cheongmicheon (b) sites.

Table 3. A comparison of the error statistics of the ET products from the MODIS, neural network and Priestley–Taylor methods for the mixed forest and paddy rice areas.

Error	MODIS		Neural network ET		Priestley–Taylor ET	
	Forest	Rice	Forest	Rice	Forest	Rice
Correlation coefficient (r)	0.847	0.791	0.958	0.703	0.620	0.302
RMSE (mm day^{-1})	0.650	1.827	0.355	0.937	2.920	2.252
MBE (mm day^{-1})	0.009	1.125	0.042	-0.605	2.602	1.610

network weight values and structures from the SMK site without retraining the neural network over CFK. Figure 2(b) shows the ET (red circles) estimated from the LM-BP neural network, MODIS ET products (blue circles) and Priestley–Taylor ET (grey circles) over the rice paddy study area. Although the neural-network-based ET and MODIS ET had opposite distributions, the accuracy was reasonable when compared with the Priestley–Taylor ET. MODIS ET had a positive bias value of $1.125 \text{ mm day}^{-1}$, whereas the neural-network-based ET had a negative MBE ($-0.605 \text{ mm day}^{-1}$), as shown in Table 3. We inferred that the accuracy of the rice paddy ET was reasonable without retraining the network with spatially dependent input parameters, which are useful for reflecting the spatial variation in different vegetation types, similar to integrating remote sensing and biophysical models. Additionally, the rice paddy environment, which had simple vegetation structure and flat terrain compared with the forest, enabled an accurate estimate of the ET despite not training the neural network.

Figure 3 shows the temporal variation in the ET products derived from the eddy flux (black line), neural network (red dash-dot line) and MODIS (blue dashed line) over the

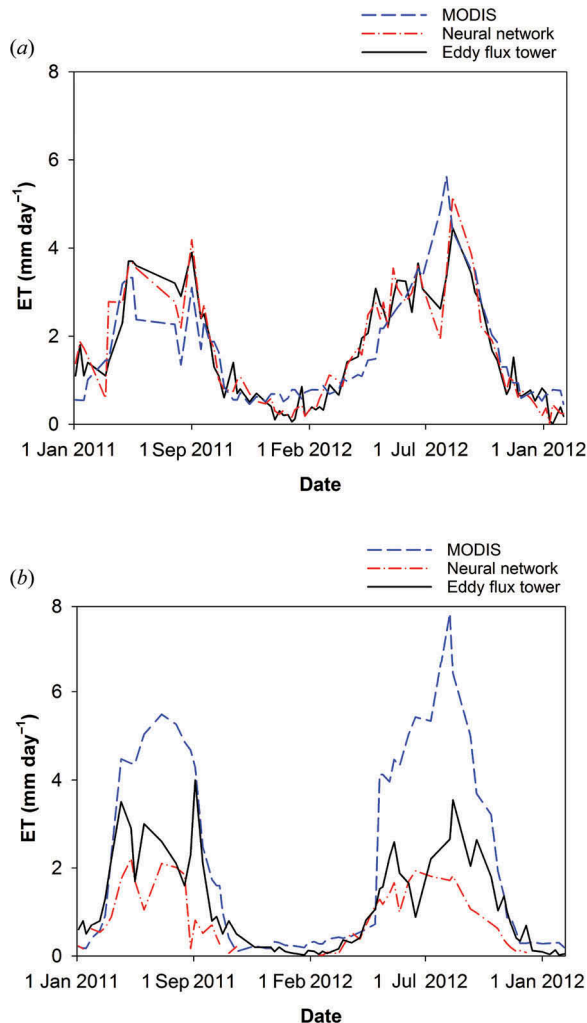


Figure 3. Temporal variation in ET from flux tower, neural network and MODIS products over the Seolmacheon (a) and Cheongmicheon (b) sites.

Seolmacheon (Figure 3(a)) and Cheongmicheon (Figure 3(b)) sites. As shown in Figure 3(a), the seasonal pattern of ET from the neural network has trends similar to those of the eddy flux tower measurements. Especially for the summer season, and despite the rainy monsoon period in the study area, ET from the neural network well describes the ground measurement because hourly based insolation from COMS MI is effective for retrieval of ET. Although MODIS ET products also well trace the variation in eddy flux tower ET, there are some discrepancy periods, especially during summer. These discrepancies between MODIS ET and eddy flux measurement would have resulted from the high rate of cloudiness during the rainy summer season, which hampers the acquisition of surface spectral information by optical satellites. All of the ET products show the seasonal pattern remarkably well, indicating that summer has the highest ET values due to the rapid growing period for vegetation, and that winter has the lowest values because of the dry and cold weather condition. In the study area, the summer season usually has not only high incident irradiation but also rainy monsoon conditions. These weather conditions are optimal for forest growth, resulting in high plant transpiration. Furthermore, during the rainy summer season, the high precipitation value over the forest area plays a source role in the evaporative conversion of surface water to water vapour.

Figure 3(b) shows that the rice paddy displayed similar seasonal patterns for all ET products, which had the highest values in summer and the lowest in winter. In the case of MODIS (blue dashed line), overestimated patterns are shown when compared with the eddy correlation measurement ET values (black line). Although the neural network ET (red dash-dot line) has underestimated values, its seasonal variation is reasonable. Although the problem of the spatial representativeness of the neural network ET emerges with different land cover types, the feasibility of the neural network ET for spatial representativeness is demonstrated.

4. Summary and conclusions

Despite the use of the combination of the conventional methods and MODIS data, the accuracy of ET estimation over regional areas still needs to be improved because it is difficult to represent the local environment using a global spatial-scale ET product. The LM-BP-based neural network approach presented here successfully estimated ET products with high accuracy when compared with previous studies (Yuan et al. 2010; Mu, Zhao, and Running 2011). In the present study, value-added products from polar-orbit and geostationary satellites were used to retrieve ET and its seasonal variation using ground station eddy flux measurements. The statistical results, such as RMSE and MBE, showed good results when compared with eddy flux-based ET measurements. Considering temporal variation, the neural-network-based ET showed variation more similar to eddy flux ET measurements than did MODIS ET products. To examine the spatial representativeness of the neural network, it was applied to a rice paddy site, and it gave reasonable results without retraining the network due to the spatially dependent input parameters. Consequently, ET estimation from a neural network should be considered as an alternative method to retrieve ET over a regional area with value-added satellite products. Nevertheless, the reliability of the results of the neural network ET has two limitations: (1) the problem of spatial representativeness of neural networks remains, although the spatially dependent input parameters gave reasonable results over the rice paddy, which has a simple vegetation structure and flat terrain; and (2) despite the outstanding performance of the neural network on a regional scale, errors inherent to the eddy correlation measurement should be considered carefully, as propagated error from eddy correlation measurements could affect the output results of the neural network model. According to Allen et al. (2011), typical errors in eddy correlation measurements are between 10% and 30%. In this study, we assumed that the eddy correlation measurements were true values to determine neuron weights similar to the general

ET. Future work will handle the spatial representativeness and propagating error of the eddy correlation measurements by considering various land cover types and the systemic characteristics of eddy flux measurements for accurate ET estimation.

Acknowledgements

We thank anonymous reviewers for providing valuable comments on this study.

Disclosure statement

No potential conflict of interest was reported by the authors.

Funding

This work was supported by 'PE15040' project funded by Korea Polar Research Institute (KOPRI).

References

- Allen, R. G., L. S. Pereira, T. A. Howell, and M. E. Jensen. 2011. "Evapotranspiration Information Reporting: I. Factors Governing Measurement Accuracy." *Agricultural Water Management* 98: 899–920. doi:10.1016/j.agwat.2010.12.015.
- Cincotti, S., A. Marchesi, and A. Serri. 1996. "Neural Network Modelling of Variable Hysteretic Inductors." *Electronics Letters* 32 (12): 1054–1055. doi:10.1049/el:19960708.
- Coulibaly, P., F. Anctil, and B. Bobée. 2000. "Daily Reservoir Inflow Forecasting Using Artificial Neural Networks with Stopped Training Approach." *Journal of Hydrology* 230: 244–257. doi:10.1016/S0022-1694(00)00214-6.
- Gao, B. C. 1996. "NDWI: A Normalized Difference Water Index for Remote Sensing of Vegetation Liquid Water from Space." *Remote Sensing of Environment* 58 (3): 257–266. doi:10.1016/S0034-4257(96)00067-3.
- Gao, Y., D. Long, and Z. L. Li. 2008. "Estimation of Daily Actual Evapotranspiration from Remotely Sensed Data under Complex Terrain over the Upper Chao River Basin in North China." *International Journal of Remote Sensing* 29 (11): 3295–3315. doi:10.1080/01431160701469073.
- Goyal, R. K. 2004. "Sensitivity of Evapotranspiration to Global Warming: A Case Study of Arid Zone of Rajasthan (India)." *Agricultural Water Management* 69 (1): 1–11. doi:10.1016/j.agwat.2004.03.014.
- Han, K. S., A. A. Viau, and F. Anctil. 2004. "An Analysis of GOES- and Noaa-Derived Land Surface Temperatures Estimated over a Boreal Forest." *International Journal of Remote Sensing* 25 (21): 4761–4780. doi:10.1080/01431160410001680446.
- Heermann, D. F., G. J. Harrington, and K. M. Stahl. 1985. "Empirical Estimation of Daily Clear Sky Solar Radiation." *Journal of Climate and Applied Meteorology* 24 (3): 206–214. doi:10.1175/1520-0450(1985)024<0206:EEODCS>2.0.CO;2.
- Isikwue, B. C., A. N. Amah, and P. O. Agada. 2012. "Empirical Model for the Estimation of Global Solar Radiation in Makurdi, Nigeria." *Physics & Space Science* 12 (1): 59–61.
- Kaminsky, E. J., H. Barad, and W. Brown. 1997. "Textural Neural Network and Version Space Classifiers for Remote Sensing." *International Journal of Remote Sensing* 18 (4): 741–762. doi:10.1080/014311697218737.
- Kawamura, H., S. Tanahashi, and T. Takahashi. 1998. "Estimation of insolation over the Pacific Ocean off the Sanriku Coast." *Journal of Oceanography* 54: 457–464. doi:10.1007/BF02742448.
- Kizu, S. 1998. "Systematic Errors in Estimation of Insolation by Empirical Formulas." *Journal of Oceanography* 54: 165–177. doi:10.1007/BF02751692.
- Korzoun, V. I., and A. A. Sokolov. 1978. "World Water Balance and Water Resources of the Earth." *Water Management and Development* 1: 2199–2215.
- L'vovich, M. I., G. F. White, A. V. Belyaev, J. Kindler, N. I. Koronkevic, T. R. Lee, and G. V. Voropaev. 1990. "Use and Transformation of Terrestrial Water Systems." In *The Earth as Transformed by Human Action: Global and Regional Changes in the Biosphere over the Past 300 Years*, edited by B. L. Turner, 235–252, Cambridge: Cambridge University Press.
- Levenberg, K. 1944. "A Method for the Solution of Certain Problems in Least Squares." *Quarterly of Applied Mathematics* 2: 164–168.

- Lucht, W., C. B. Schaaf, and A. H. Strahler. 2000. "An Algorithm for the Retrieval of Albedo from Space Using Semiempirical BRDF Models." *IEEE Transactions on Geoscience and Remote Sensing* 38 (2): 977–998. doi:10.1109/36.841980.
- Marquardt, D. 1963. "An Algorithm for Least-Squares Estimation of Nonlinear Parameters." *Journal of the Society for Industrial and Applied Mathematics* 11 (2): 431–441. doi:10.1137/0111030.
- Mu, Q., M. Zhao, and S. W. Running. 2011. "Improvements to a MODIS Global Terrestrial Evapotranspiration Algorithm." *Remote Sensing of Environment* 115 (8): 1781–1800. doi:10.1016/j.rse.2011.02.019.
- Prechelt, L. 1998. "Automatic Early Stopping Using Cross Validation: Quantifying the Criteria." *Neural Networks* 11 (4): 761–767. doi:10.1016/S0893-6080(98)00010-0.
- Priestley, C. H. B., and R. J. Taylor. 1972. "On the Assessment of Surface Heat Flux and Evaporation Using Large-Scale Parameters." *Monthly Weather Review* 100 (2): 81–92. doi:10.1175/1520-0493(1972)100<0081:OTAOSH>2.3.CO;2.
- Roujean, J. L., M. Leroy, and P. Y. Deschamps. 1992. "A Bidirectional Reflectance Model of the Earth's Surface for the Correction of Remote Sensing." *Journal of Geophysical Research* 97 (D18): 20455–20468. doi:10.1029/92JD01411.
- Rouse, J. W., R. H. Haas, J. A. Schell, and D. W. Deering. 1974. "Monitoring Vegetation Systems in the Great Plains with ERTS." In *Proceedings, Third Earth Resources Technology Satellite-1 Symposium, Greenbelt: NASA-SP-351*, edited by S. C. Freden, E. P. Mercanti, and M. A. Becker, 310–317. Washington, DC: NASA.
- Sánchez, J. M., V. Caselles, R. Nicolós, E. Valor, C. Coll, and T. Laurila. 2007. "Evaluation of the B-Method for Determining Actual Evapotranspiration in a Boreal Forest from MODIS Data." *International Journal of Remote Sensing* 28 (6): 1231–1250. doi:10.1080/01431160600928617.
- Schaaf, C. B., F. Gao, A. H. Strahler, W. Lucht, X. Li, T. Tsang, N. C. Strugnell, X. Zhang, Y. Jin, J. P. Muller, P. Lewis, M. Barnsley, P. Hobson, M. Disney, G. Roberts, M. Dunderdale, C. Doll, R. d'Entremont, B. Hu, S. Liang, J. L. Privette, and D. Roy. 2002. "First Operational BRDF, Albedo and Nadir Reflectance Products from MODIS." *Remote Sensing of Environment* 83 (1–2): 135–148. doi:10.1016/S0034-4257(02)00091-3.
- Sun, Z., M. Gebremichael, J. Ardö, A. Nickless, B. Caquet, L. Merboldh, and W. Kutsch. 2012. "Estimation of Daily Evapotranspiration over Africa Using Modis/Terra and SEVIRI/MSG Data." *Atmospheric Research* 112: 35–44. doi:10.1016/j.atmosres.2012.04.005.
- Vermote, E. F., D. Tanre, J. L. Deuze, M. Herman, and J. J. Morcette. 1997. "Second Simulation of the Satellite Signal in the Solar Spectrum, 6S: An Overview." *IEEE Transactions on Geoscience and Remote Sensing* 35 (3): 675–686. doi:10.1109/36.581987.
- Wan, Z., Y. Zhang, Q. Zhang, and Z.-L. Li. 2002. "Validation of the Land-Surface Temperature Products Retrieved from Terra Moderate Resolution Imaging Spectroradiometer Data." *Remote Sensing of Environment* 83 (1–2): 163–180. doi:10.1016/S0034-4257(02)00093-7.
- Wanchang, Z., Y. Yamaguchi, and K. Ogawa. 2000. "Evaluation of the Effect of Pre-processing of the Remotely Sensed Data on the Actual Evapotranspiration, Surface Soil Moisture Mapping by an Approach Using Landsat, DEM and Meteorological Data." *Geocarto International* 15 (4): 59–70. doi:10.1080/10106040008542173.
- Wang, K., and R. E. Dickinson. 2012. "A Review of Global Terrestrial Evapotranspiration: Observation, Modeling, Climatology, and Climatic Variability." *Reviews of Geophysics* 50 (2): 19–24. doi:10.1029/2011RG000373.
- Yeom, J. M., and K. S. Han. 2010. "Improved Estimation of Surface Solar Insolation Using a Neural Network and MTSAT-IR Data." *Computers & Geosciences* 36 (5): 590–597. doi:10.1016/j.cageo.2009.08.012.
- Yeom, J. M., K. S. Han, Y. S. Kim, and J. D. Jang. 2008. "Neural Network Determination of Cloud Attenuation to Estimate Insolation Using MTSAT-IR Data." *International Journal of Remote Sensing* 29 (21): 6193–6208. doi:10.1080/01431160802175421.
- Yu, H., and B. M. Wilamowski. 2011. "Levenberg-Marquardt Training." In *Industrial Electronics Handbook*, edited by M. Bogdan, J. Wilamowski, and D. Irwin, 1–15. Boca Raton, FL: CRC Press.
- Yuan, W., S. Liu, G. Yu, J.-M. Bonnefond, J. Chen, K. Davis, A. R. Desai, A. H. Goldstein, D. Gianelle, F. Rossi, A. E. Suyker, and S. B. Verma. 2010. "Global Estimates of Evapotranspiration and Gross Primary Production Based on MODIS and Global Meteorology Data." *Remote Sensing of Environment* 114 (7): 1416–1431. doi:10.1016/j.rse.2010.01.022.